eprints@whiterose.ac.uk
https://eprints.whiterose.ac.uk/

Cationic sterically-stabilized diblock copolymer nanoparticles exhibit exceptional tolerance towards added salt

Sarah J. Byard[1], Adam Blanazs,[2] John F. Miller[3] and Steven P. Armes[1]*

1. Department of Chemistry, University of Sheffield, Brook Hill, Sheffield, South Yorkshire, S3 7HF, UK.

2. BASF SE, GMV/P - B001, 67056 Ludwigshafen, Germany.

3. Enlighten Scientific LLC, Hillsborough NC 27278, USA.

Abstract. For certain commercial applications such as enhanced oil recovery, sterically-stabilized colloidal dispersions that exhibit high tolerance towards added salt are desirable. Herein we report a series of new cationic diblock copolymer nanoparticles that display excellent colloidal stability in concentrated aqueous salt solutions. More specifically, poly(2-(acryloyloxy)ethyl trimethylammonium chloride) (PATAC) has been chain-extended by reversible addition-fragmentation chain transfer (RAFT) aqueous dispersion polymerization of diacetone acrylamide (DAAM) at 70 °C to produce $PATAC_{100}$-$PDAAM_x$ diblock copolymer spheres at 20 % w/w solids via polymerization-induced self-assembly (PISA). Transmission electron microscopy (TEM) and dynamic light scattering (DLS) analysis confirm that the mean sphere diameter can be adjusted by systematic variation of the mean degree of polymerization of DAAM. Remarkably, DLS studies confirm that highly cationic $PATAC_{100}$-$PDAAM_{1500}$ spheres retain their colloidal stability in the presence of either 4.0 M KCl or 3.0 M ammonium sulfate for at least 115 days at 20 ˚C. The mole fraction of PATAC chains within the stabilizer shell was systematically varied by chain extension of various binary mixtures of non-ionic and PATAC with DAAM to produce ([n] $PATAC_{100}$ + [1-n] $PDMAC_{67}$)-$PDAAM_z$ diblock copolymer spheres at 20 % w/w. DLS studies confirmed that a relatively high mole fraction of cationic PATAC stabilizer chains (n $\geq$ 0.75) is required for the dispersions to remain colloidally stable in 4.0 M KCl. Cationic worms and vesicles could also be synthesized by using a binary mixture of PATAC and PDMAC precursors where n = 0.10. However, the vesicles only remained colloidally stable up to 1.0 M KCl, whereas the worms proved to be stable up to 2.0 M KCl. Such block copolymer nanoparticles are expected to be useful model systems for understanding the behavior of aqueous colloidal dispersions in extremely salty media. Finally, zeta potentials determined using electrophoretic light scattering (ELS) are presented for nanoparticles dispersed in highly salty media.

* Author to whom correspondence should be addressed (s.p.armes@shef.ac.uk)

Introduction. It has been recognized for more than a century that charge-stabilized colloidal particles can aggregate in the presence of salt.[1,2] This phenomenon can be explained in terms of Deryaguin-Landau-Verwey-Overbeek (DLVO) theory[3,4] and is commercially exploited for the industrial manufacture of latex gloves.[5] Faraday was the first to demonstrate that protein-stabilized particles typically exhibit significantly better colloidal stability in the presence of added salt: indeed, some of his gelatin-coated gold sols remain stable more than 160 years after their synthesis.[6] For certain applications such as enhanced oil recovery, colloidal dispersions that can exhibit extreme salt tolerance at both ambient and elevated temperature are desirable.[7–13]

Recently, various polyelectrolytes have been used to simulatenouly confer both charge and steric stabilization (so-called electrosteric stabilization) onto inorganic particles for such high salt applications. For example, Bagaria et al. physically adsorbed random and block copolymers comprising 2-methyl-2-acrylamidopropanesulfonate (AMPS) and acrylic acid (AA) onto the surface of ~100 nm iron oxide nanoparticles.[9] For example, poly(AMPS-stat-AA)-coated iron nanoparticles remained colloidally stable in a mixture of 1.4 M NaCl and 0.2 M $CaCl_2$ at both room temperature and 90 °C for up to 1 month. In a later publication, the same team showed that iron nanoparticles resisted aggregation in a mixture of 1.4 M NaCl and 0.2 M $CaCl_2$ if poly(AMPS-stat-AA) chains were grafted onto the nanoparticle surface.[10]

Similarly, salt-tolerant polymer latexes have been synthesized by free radical aqueous dispersion polymerization. For example, Cho et al. prepared submicrometer-sized polyacrylamide particles in the presence of 1.8 - 2.3 M ammonium sulfate. The particles were sterically-stabilized by a cationic homopolyelectrolyte known as poly(2-(acryloyloxy)ethyltrimethylammonium chloride) or PATAC.[14] In closely-related work, Aijun et al. reported the preparation of colloidally stable, cationic latex particles in the presence of 1.9 - 2.5 M ammonium sulfate via aqueous dispersion copolymerization of acrylamide with 2-

(methacryloyloxy)ethyltrimethylammonium chloride) (MATAC), again using PATAC as the steric stabilizer.[15]

Thus far, the morphology of salt-tolerant polymer particles has been confined to spheres. This is no doubt because such formulations are typically based on conventional free radical polymerization. In contrast, controlled radical polymerization techniques such as RAFT polymerization enable the synthesis of well-defined, functional diblock copolymers.[16–27] Moreover, it is now well-established that, by choosing a suitable selective solvent, a range of diblock copolymer nano-objects can be prepared in the form of concentrated aqueous dispersions via RAFT-mediated polymerization-induced self-assembly (PISA).[28–36]

In a previous publication,[37] we reported the preparation and characterization of a series of PDMAC-PDAAM diblock copolymer nano-objects synthesized via RAFT aqueous dispersion polymerization. Moreover, post-polymerization reaction of the pendent ketone group on the DAAM residues with adipic acid dihydrazide was demonstrated. Such crosslinking allows covalently-stabilized nano-objects to be produced in the form of concentrated aqueous dispersions.

Herein, this latter PISA formulation has been modified by incorporating PATAC as either the sole or supplementary cationic steric stabilizer block. Accordingly, a binary mixture of PDMAC and PATAC homopolymer precursors was chain-extended with DAAM via RAFT aqueous dispersion copolymerization to produce ([n] $PATAC_x$ + [1-n] $PDMAC_y$)-$PDAAM_z$ diblock copolymer nanoparticles, where n denotes the mole fraction of PATAC and x, y and z denote the mean degree of polymerization (DP) for the PATAC, PDMAC and PDAAM blocks, respectively. Pure sphere, worm and vesicle morphologies could be obtained depending on the precise PISA formulation. The effect of varying n (for a fixed x, y and z) on the cationic character of spherical nanoparticles has been studied. Moreover, the effect of increasing the

PDAAM DP on the mean diameter has been investigated for a series of $PATAC_{100}$-$PDAAM_z$ spheres. DLS has been used to study the colloidal stability of these new diblock copolymer nanoparticles in concentrated aqueous solutions of either KCl or ammonium sulfate. We report for the first time the use of a next-generation electrophoretic light scattering (ELS) instrument to determine zeta potentials for nanoparticles dispersed in highly salty media.

Experimental

Materials

N,N-Dimethylacrylamide (DMAC), 2-(dodecylthiocarbonothioylthio)-2-methylpropionic acid (DDMAT), dioxane and 2,2′-asobis(2-methylpropionamidine) dihydrochloride (AIBA) were purchased from Sigma-Aldrich UK and used as received. Diacetone acrylamide (DAAM), 4-dimethylaminopyridine (DMAP), N,N'-dicyclohexylcarbodiimide (DCC) and adipic acid dihydrazide (ADH) were purchased from Alfa Aesar (UK) and were used as received. 2,2′-Asobis(2-methylpropionitrile) (AIBN) was purchased from Molekula (UK) and was used as received. 2,2'-Asobis[2-(2-imidasolin-2-yl)propane] dihydrochloride (VA-044) initiator was purchased from Wako Chemicals (Japan) and was used as received. Diethyl ether, potassium chloride and ammonium sulfate were purchased from VWR Chemicals. Dichloromethane, methanol and acetonitrile were purchased from Fisher Scientific (UK). All solvents were HPLC-grade and deuterated methanol was purchased from Cambridge Isotope Laboratories (UK). Finally, 2-(acryloyloxy)ethyltrimethylammonium chloride (ATAC) was kindly donated by BASF (Germany) in the form of an 80 % w/w aqueous solution.

Synthesis

Methylation of 2-(dodecylthiocarbonothioylthio)-2-methylpropionic acid (DDMAT)

DDMAT (4.30 g, 11.8 mmol) was dissolved in anhydrous dichloromethane (30 mL) in a 100 mL round-bottomed flask, which was cooled to 0 °C by immersion in an ice bath. DMAP (0.29

g, 2.4 mmol) and excess anhydrous methanol (2.0 g) were added to the stirred solution at 0 °C. DCC (2.72 g, 13.2 mmol) was added gradually over 5 min. This reaction solution was allowed to warm up to 20 °C and stirred continuously for 16 h at this temperature prior to filtration to remove the insoluble dicyclohexyl urea side-product. Column chromatography was used to purify the product using dichloromethane as the eluent. This solvent was removed under vacuum to afford methyl 2-(dodecylthiocarbonothioylthio)-2-methylpropionate (Me-DDMAT) as an orange oil (4.21 g, 94%). ^{1}H NMR spectroscopy studies indicated a degree of esterification of 97 % (see Figure S1).

Synthesis of poly(N,N-dimethylacrylamide) (PDMAC) via RAFT solution polymerization

A typical protocol for the synthesis of a $PDMAC_{67}$ precursor was conducted as follows. Me-DDMAT (2.00 g, 5.30 mmol), AIBN (87.0 mg 0.53 mmol, Me-DDMAT/AIBN molar ratio = 10), and DMAC (34.12 g, 0.34 mol) were weighed into a 500 mL round-bottomed flask. Dioxane (84.5 mL) was added to produce a 30% w/w solution, which was purged with nitrogen for 1 h. The sealed flask was immersed into an oil bath set at 70 °C for 25 min and the polymerization was subsequently quenched by immersing the flask in an ice bath, followed by exposure of its contents to air. The final DMAC conversion was 95%, as judged by ^{1}H NMR spectroscopy. The crude polymer was purified by precipitation into a ten-fold excess of diethyl ether (twice). The resulting purified PDMAC was isolated by filtration and dissolved in deionized water, any residual diethyl ether/dioxane was removed under reduced pressure and the aqueous solution was freeze-dried for 48 h to produce a yellow solid. End-group analysis using UV spectroscopy indicated a mean degree of polymerization of 67 (the Beer-Lambert plot for Me-DDMAT is provided in Figure S2). DMF GPC analysis indicated an M_n of 7 400 g mol^{-1} and an M_w/M_n of 1.14. A $PDMAC_{37}$ was also prepared using the same protocol. In this case DMF GPC analysis indicated an M_n of 3 400 g mol^{-1} and an M_w/M_n of 1.15.

Synthesis of poly(2-(acryloyloxy)ethyl trimethylammonium chloride) (PATAC) via RAFT solution polymerization

A typical protocol for the synthesis of a PATAC$_{100}$ precursor was conducted as follows. Me-DDMAT (0.600 g, 1.58 mmol), VA-044 (0.10 g 0.317 mmol, Me-DDMAT/AIBN molar ratio = 5.0), and 2-(acryloyloxy)ethyl trimethylammonium chloride (ATAC) (30.69 g, 0.13 mol, supplied as an 80% aqueous solution) were weighed into a 250 mL round-bottomed flask. Methanol (94.45 mL) and water (0.43 mL) were added to produce a 20% w/w solution, which was purged with nitrogen for 1 h. The sealed flask was immersed into an oil bath set at 44 °C for 2 h and the polymerization was subsequently quenched by immersing the flask in ice, followed by exposure to air. The final ATAC conversion was 96%, as judged by ^{1}H NMR spectroscopy. Methanol was removed under reduced pressure, followed by purification of the polymer by precipitation into a ten-fold excess of acetonitrile. The precipitate was redissolved in water and precipitated once more into excess acetonitrile. The purified PATAC was dissolved in deionized water, any residual solvent was removed under reduced pressure, and the resulting aqueous solution was freeze-dried for 48 h to produce a yellow solid. End-group analysis using UV spectroscopy indicated a mean degree of polymerization of 100. Aqueous GPC analysis indicated an M_n of 29 500 g mol^{-1} and an M_w/M_n of 1.19, respectively. A PATAC$_{91}$ precursor was prepared using the same protocol. Aqueous GPC analysis indicated an M_n of 25 800 g mol^{-1} and an M_w/M_n of 1.14.

Synthesis of (0.9 PDMAC$_{67}$ + 0.1 PATAC$_{100}$)-PDAAM$_{1500}$ diblock copolymer spheres by RAFT aqueous dispersion polymerization

The synthesis of (0.9 PDMAC$_{67}$ + 0.1 PATAC$_{100}$)-PDAAM$_{1500}$ spheres at 20% w/w solids is representative and was conducted as follows. PDMAC$_{67}$ precursor (0.80 g, 0.114 mmol), PATAC$_{100}$ precursor (0.250 g, 0.013 mmol), AIBA initiator (3.40 mg, 0.013 mmol, [PDMA$_{67}$

+ $PATAC_{100}$]/AIBA molar ratio = 10) and DAAM monomer (32.1 g, 0.19 mol; target DP = 1500) were weighed into a 250 mL round-bottomed flask. Deionized water (131.8 mL) was then added to afford a 20% w/w aqueous solution, which was degassed for 1 h at 4 °C prior to immersion in an oil bath set at 56 °C. This reaction solution was stirred for 18 h and then the polymerization was quenched by exposure to air. The DAAM monomer conversion was more than 99% as judged by ^{1}H NMR spectroscopy. All other PISA syntheses were conducted at 20 % w/w solids using the same protocol.

Polymer Characterization

^{1}H NMR Spectroscopy

All NMR spectra were recorded in CD_3OD using a 400 MHz Bruker Avance III HD 400 spectrometer at 25 °C. Typically, 64 scans were acquired to ensure high-quality spectra.

End-Group Analysis via UV Spectroscopy

UV−visible absorption spectra were recorded between 200 and 800 nm using a PC-controlled UV-1800 spectrophotometer operating at 25 °C and equipped with a 1 cm path length quartz cell. A Beer-Lambert curve was constructed using a series of eighteen Me-DDMAT stock solutions of varying concentration in methanol. The absorption maximum at 308 nm assigned to the trithiocarbonate end-group[38] was used for this calibration plot, and Me-DDMAT concentrations were selected such that the absorbance always remained below unity. The mean DPs for the PDMAC and PATAC stabilizers were determined using the molar extinction coefficient of $15\,740 \pm 8$ $mol^{-1}\,dm^3\,cm^{-1}$ calculated for Me-DDMAT.

Gel Permeation Chromatography (GPC)

The molecular weight distribution for the PATAC stabilizer block was assessed using aqueous GPC. An acidic aqueous buffer containing 0.5 M acetic acid and 0.3 M NaH_2PO_4 was adjusted

to pH 2 using concentrated HCl and used as an eluent for aqueous GPC analysis of the cationic PATAC precursor. The GPC instrument comprised an Agilent 1260 Infinity series degasser and pump, two Agilent PL 8 µm Aquagel-OH 30 columns and one 8 µm Aquagel-OH 40 column in series. These columns were calibrated using ten near-monodisperse poly(ethylene oxide) standards ranging from 1 080 g mol^{-1} to 905 000 g mol^{-1}. A refractive index detector operating at 30 °C was used at a flow rate of 1.0 mL min^{-1}. Chromatograms were analyzed using Agilent GPC/SEC software.

The molecular weight distributions of the PDMAC$_{67}$ stabilizer block and a PDMAC-PDAAM diblock copolymer were assessed using DMF GPC. The GPC instrument comprised two Agilent PL gel 5 µm Mixed-C columns and a guard column connected in series to an Agilent 1260 Infinity GPC system equipped with both refractive index and UV−visible detectors (only the refractive index detector was used) operating at 60 °C. The GPC eluent was HPLC-grade DMF containing 10 mM LiBr at a flow rate of 1.0 mL min^{-1} and DMSO was used as a flow-rate marker. Calibration was achieved using a series of ten near-monodisperse poly(methyl methacrylate) standards (ranging in M_p from 625 to 618 000 g mol^{-1}). Chromatograms were analyzed using Agilent GPC/SEC software.

Transmission Electron Microscopy (TEM)

Copper/palladium TEM grids (Agar Scientific, UK) were coated in-house to yield a thin film of amorphous carbon. The coated grids were then subjected to a glow discharge for 30 s. Individual 10.0 µL droplets of 0.1% w/w aqueous copolymer dispersions were placed on freshly-treated grids for 1 min and then carefully blotted with filter paper to remove excess solution. To ensure sufficient electron contrast, uranyl formate (9.0 µL of a 0.75% w/w solution) was absorbed onto the sample-loaded grid for 20 s and then carefully blotted to remove excess stain. Each grid was then dried using a vacuum hose. Imaging was performed

using a FEI Tecnai Spirit 2 microscope fitted with an Orius SC1000B camera operating at 80 kV.

Dynamic Light Scattering (DLS)

DLS studies were conducted using a Malvern Zetasizer NanoZS instrument at 20 °C. All measurements were made on 0.1% w/w aqueous copolymer dispersions in 1.0 cm cuvette cells; scattered light was detected at 173° and data were averaged over three consecutive runs. Sphere-equivalent intensity-average diameters were calculated for diblock copolymer nano-objects via the Stokes−Einstein equation, which assumes perfectly monodisperse, non-interacting spheres. According to its manufacturer, this Nano ZS instrument set-up has an upper limit particle diameter of approximately 6 µm. The solution viscosity was taken to be that of pure water for nanoparticles prepared in 1 mM KCl. For DLS studies performed in the presence of higher salt concentrations, the solution viscosity was calculated for each salt concentration using literature data (see Table S1 in the Supporting Information).[39]

Aqueous Electrophoresis

Zeta potential measurements were performed using two different ELS instruments. Electrophoretic mobilities were determined for 0.1% w/w aqueous copolymer dispersions at 25 °C in the presence of 1 mM KCl using the Malvern Zetasizer Nano ZS instrument described above using its default settings and a palladium Uzgiris-type dip electrode.[40] However, such conventional commercial instruments do not allow accurate electrophoretic mobilities to be measured at ionic strengths above 100 mM. Thus, a Next Generation Electrophoretic Light Scattering system[41] (NG-ELS; Enlighten Scientific LLC, Hillsborough, NC, USA) was used to conduct further measurements at both low and high salt. NG-ELS is an upgraded version of the original phase analysis light scattering (PALS) instrument[42]. PALS has become the de facto method to estimate zeta potentials using ELS at high salt concentrations. However, it assumes

that the nanoparticles have discrete electrophoretic mobilities, i.e. there is no distribution in mobility. The more conventional laser Doppler electrophoresis (LDE) method can provide the distribution information but only at lower salt concentrations. In the absence of any meaningful distribution information, ELS measurements are prone to misinterpretation owing to problems such as aggregation, thermal convection and additional light scattering by particulate contaminants (e.g. dust). NG-ELS employs both the PALS and LDE signal processing at high salt concentrations and enables quantitative measurement of electrode polarization in order to accurately determine the applied electric field during the electrophoresis measurements. Platinized platinum electrodes[43] were used to minimize undesirable electrode-solution interface phenomena such as electrolysis. Both instruments use the Smoluchowski model to calculate zeta potentials from electrophoretic mobilities.[44]

RESULTS AND DISCUSSION

Synthesis of PDMAC and PATAC homopolymer precursors via RAFT solution polymerization

The RAFT solution polymerization of ATAC was conducted in a 94:6 methanol/water mixture at 44 °C using Me-DDMAT as the RAFT agent, as outlined in Figure 1. PATAC homopolymers were prepared with mean degrees of polymerization (DPs) of either 91 or 100, as determined by end-group analysis using UV spectroscopy. Aqueous GPC analysis indicated narrow molecular weight distributions ($M_w/M_n < 1.19$) for these precursors, see Figure S3a. The RAFT solution polymerization of DMAC was conducted in dioxane at 70 °C using Me-DDMAT as the RAFT agent, as outlined in Figure 1. PDMAC homopolymers were prepared with DPs of 37 and 67, as determined by end-group analysis using UV spectroscopy. DMF GPC analysis indicated narrow molecular weight distributions ($M_w/M_n < 1.15$) for these precursors, see Figure S3b.

RAFT Aqueous Dispersion Polymerization of DAAM

A series of ([n] $PATAC_x$ + [1-n] $PDMAC_y$)-$PDAAM_z$ diblock copolymer nanoparticles were synthesized by simultaneous chain extension of a binary pair of PATAC and PDMAC precursors via RAFT aqueous dispersion polymerization of DAAM at 56 °C, see Figure 1. These PISA syntheses were conducted at 20% w/w solids and the PATAC DP was selected to be significantly longer than that of the PDMAC block to ensure that the former stabilizer would exert a significant effect over the electrophoretic footprint of these block copolymer nano-objects even when present as a minor fraction. Given that the PATAC and PDMAC precursors were prepared using the same RAFT agent, the kinetics for the ensuing DAAM polymerization were expected to be identical for these two steric stabilizer blocks. Experiments for which n = 0 or n = 1 were also conducted to provide diblock copolymer nano-objects with either zero or maximum cationic character, respectively. DAAM conversions of more than 99 % were routinely achieved for such PISA syntheses as determined by ^{1}H NMR spectroscopy studies conducted in CD_3OD (i.e., complete disappearance of the vinyl signals at 5.4−6.4 ppm assigned to DAAM monomer, see Figure S4). Unfortunately, GPC analysis could not be conducted on the PATAC-PDAAM diblock copolymer because no suitable eluent could be identified that would solubilize the cationic PATAC and the hydrophobic PDAAM blocks. The same problem was also encountered for the GPC analysis of nanoparticles comprising binary mixtures of PATAC-PDAAM and PDMAC-PDAAM diblock copolymer chains. However, GPC analysis of the neutral $PDMAC_{67}$-$PDAAM_{1500}$ diblock copolymer chains (i.e., for n = 0) indicated a high blocking efficiency (minimal $PDMAC_{67}$ precursor contamination) and a relatively narrow molecular weight distribution (M_w/M_n = 1.50) see Figure 2. A summary of the characterization data obtained for all of the ([n] $PATAC_{100}$ + [1-n] $PDMAC_{67}$)-$PDAAM_z$ diblock copolymer nanoparticles prepared in this study is given in Table 1.
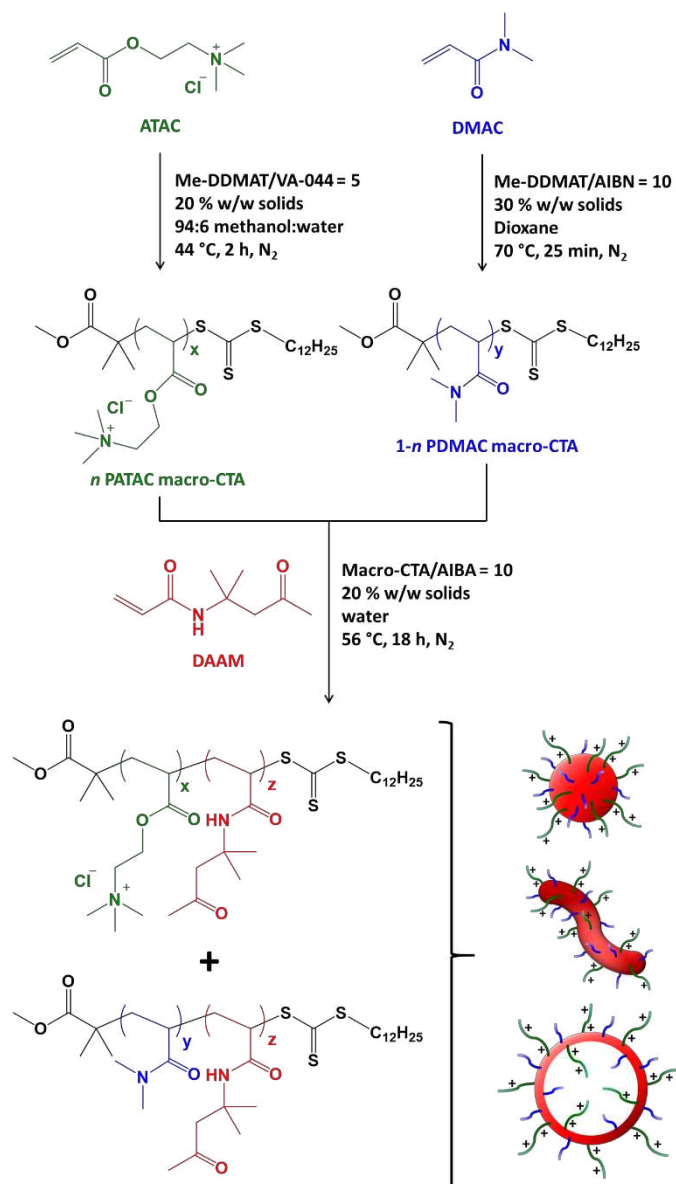
Fig. 1. Reaction scheme for the synthesis of (i) $PDMAC_x$ homopolymer (x = 37 or 67) via RAFT solution polymerization of DMAC in dioxane and (ii) $PATAC_y$ homopolymer (y = 91 or 100) via RAFT solution polymerization of ATAC in a 94:6 methanol/water mixture. Subsequent chain extension of a judicious binary mixture of these PATAC and PDMAC precursors via RAFT aqueous dispersion polymerization of DAAM to produce a series of diblock copolymer nanoparticles of tunable cationic character.
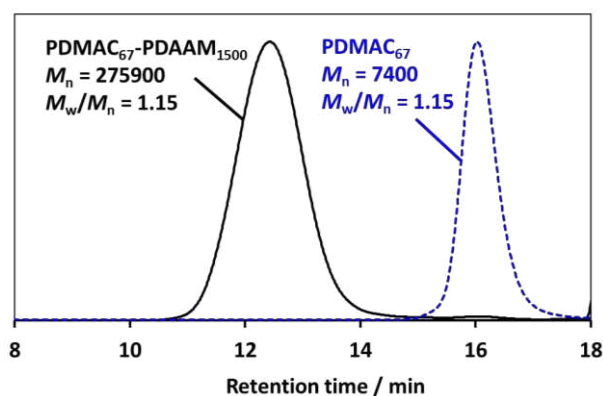
Fig. 2. DMF GPC chromatograms recorded for the PDMAC$_{67}$-PDAAM$_{1500}$ diblock copolymer and the PDMAC$_{67}$ homopolymer precursor. Refractive index detector. Calibration was achieved using a series of near-monodisperse poly(methyl methacrylate) standards.

Table 1. Summary of the characterization data obtained for the ([n] PATAC$_x$ + [1-n] PDMAC$_y$)-PDAAM$_z$ diblock copolymer nanoparticles prepared in this study.

Entry No.	x	y	z	n	DLS diameter[a] / nm	Zeta Potential[b] /mV	Assigned TEM morphology
1	100	-	100	1.00	75 ± 20	+50	Spheres
2	100	-	300	1.00	95 ± 18	+34	Spheres
3	100	-	500	1.00	97 ± 20	+35	Spheres
4	100	-	700	1.00	101 ± 17	+35	Spheres
5	100	-	1000	1.00	122 ± 20	+34	Spheres
6	100	-	1500	1.00	154 ± 44	+33	Spheres
7	100	-	2000	1.00	206 ± 45	+37	Spheres
8	-	67	1500	0.00	271 ± 111	+1	Spheres
9	100	67	1500	0.10	204 ± 32	+16	Spheres
10	100	67	1500	0.25	177 ± 29	+28	Spheres
11	100	67	1500	0.50	145 ± 22	+32	Spheres
12	100	67	1500	0.75	144 ± 19	+38	Spheres
13	91	37	90	0.10	195 ± 89	+33	Worms
14	91	67	300	0.10	196 ± 34	+40	Vesicles
15	91	67	400	0.10	194 ± 19	+37	Vesicles
16	91	67	900	0.10	221 ± 38	+34	Vesicles

[a] Intensity-average diameter determined by DLS analysis of 0.1 % copolymer dispersions at 20°C in 1mM KCl obtained using the Stokes-Einstein equation. Standard deviations were calculated using the polydispersity index (PDI) ($STD\ DEV = \sqrt{PDI} \times DLS\ diameter$).

[b] Zeta potential determined in the presence of 1 mM KCl at pH 7-8.

Nanoparticle characterization

Previously, we reported that the use of relatively long non-ionic blocks in RAFT aqueous dispersion polymerization syntheses almost invariably result in kinetically-trapped spheres.[37,45] The same constraint applies for PISA syntheses performed using polyelectrolytic stabilizer blocks regardless of their mean DP.[46–50] No doubt this is because strong mututal electrostatic repulsion between nanoparticles prevent their 1D fusion to form worms during the PISA synthesis.[28,29] Indeed, in the present study all of the $PATAC_{100}$-$PDAAM_z$ diblock copolymers (n = 1.00) formed well-defined spherical nanoparticles as determined by TEM studies, see Figure 3 for representative TEM images. Moreover, the mean particle diameter increased monotonically as the PDAAM DP (z) was systematically increased from 100 to 2000 (see entries 1-7 in Table 1). A systematic increase in intensity-average particle diameter from 75 to 206 nm was indicated by dynamic light scattering (DLS) studies performed in 1 mM KCl.
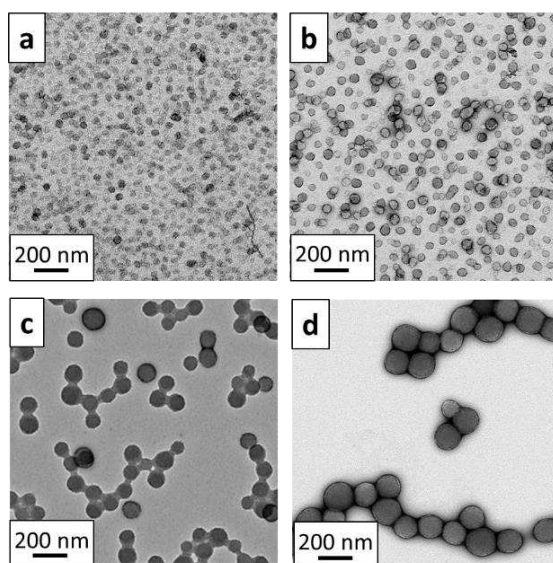

Fig. 3. Representative TEM images obtained for (a) $PATAC_{100}$-$PDAAM_{100}$ (b) $PATAC_{100}$-$PDAAM_{300}$ (c) $PATAC_{100}$-$PDAAM_{1500}$ and (d) $PATAC_{100}$-$PDAAM_{2000}$.

Zeta potential measurements were conducted on each of the seven aqueous dispersions of $PATAC_{100}$-$PDAAM_z$ spherical nanoparticles (where z = 100 – 2000) dispersed in 1 mM KCl

14

at pH 7-8, see Table 1. In each case these nanoparticles proved to be highly cationic, exhibiting zeta potentials of at least +33 mV with little or no particle size dependence.

Salt tolerance of PATAC$_{100}$-PDAAM$_{1500}$ spherical nanoparticles

A 20 % w/w aqueous dispersion of PATAC$_{100}$-PDAAM$_{1500}$ nanoparticles was diluted to 0.1 % w/w via hand-mixing for 10 min using aqueous KCl solutions ranging from 1.0 mM to 4.0 M. DLS analysis was conducted on these dispersions, see Figure 4a. DLS is strongly biased towards the presence of aggregates because the scattered light intensity scales as the sixth power of the particle radius.[51] For example, the scattered light intensity arising from nanoparticles with a mean diameter of 200 nm is 64 times greater than that for nanoparticles of 100 nm diameter. Thus it is well-known that this technique is well-suited for assessing the incipient flocculation of various types of colloidal dispersions.[52–55] In the present study, aqueous dispersions were judged to be colloidally unstable if a significant increase in their intensity-average particle diameter and DLS polydispersity index (which is expressed as a standard deviation) was observed, after correcting for the relatively high viscosity of concentrated aqueous KCl solutions compared to that of pure water (see Table S1 in the Supporting Information for a summary of the solution viscosities used in this study).[39]

The PATAC$_{100}$-PDAAM$_{1500}$ nanoparticles remained colloidally stable in the presence of 1.0 to 4.0 M KCl. In fact, a modest reduction in intensity-average particle diameter (from 154 ± 44 nm to 134 ± 53 nm in 4 M KCl) was observed compared to that obtained for the same dispersion in 1 mM KCl (entry 6, Table 1). This is attributed to the well-known polyelectrolyte effect:[56] the highly salty media ensures efficient electrostatic screening, which leads to relaxation of the initially highly stretched cationic PATAC$_{100}$ stabilizer chains and hence a thinner coronal layer.

The PATAC$_{100}$-PDAAM$_{1500}$ nanoparticles exhibited excellent resistance towards flocculation even in the presence of 4.0 M KCl (which is close to a saturated solution for this particular salt). In view of this observation, these dilute aqueous dispersions were allowed to age for 115 days at 20 ˚C with their colloidal stability being periodically monitored by DLS analysis, see Figure 4b. After almost four months under such conditions, no significant increase in apparent particle size was observed for these PATAC$_{100}$-PDAAM$_{1500}$ nanoparticles. Thus, further salt resistance studies were conducted using 1.0 to 4.0 M ammonium sulfate. The molar ionic strength of this 1:2 salt is significantly higher than that of a 1:1 electrolyte such as KCl.[57] Again, the initial 20% w/w aqueous dispersion of PATAC$_{100}$-PDAAM$_{1500}$ nanoparticles was diluted to 0.1 % w/w using up to 4.0 M ammonium sulfate prior to DLS studies, see Figure 4c.

Remarkably, colloidal stability was retained up to 3.8 M ammonium sulfate. However, aggregation was eventually observed at 3.9 M and 4.0 M, with floccs of 305 ± 269 nm and 906 ± 659 nm respectively being formed under such conditions. It is perhaps worth emphasizing that this demonstration of colloidal stability in the presence of 3.8 M ammonium sulfate compares quite favorably with several recent reports of salt-tolerant nanoparticles.[9,10,14,15]

The PATAC$_{100}$-PDAAM$_{1500}$ nanoparticles were aged for 115 days at 20 ˚C in up to 4.0 M ammonium sulfate, see Figure 4d. At the highest salt concentration, nanoparticle flocculation was observed immediately. However, nanoparticles dispersed in up to 3.0 M ammonium sulfate exhibited no significant increase in apparent particle size after 115 days, indicating high resistance towards flocculation under such conditions.
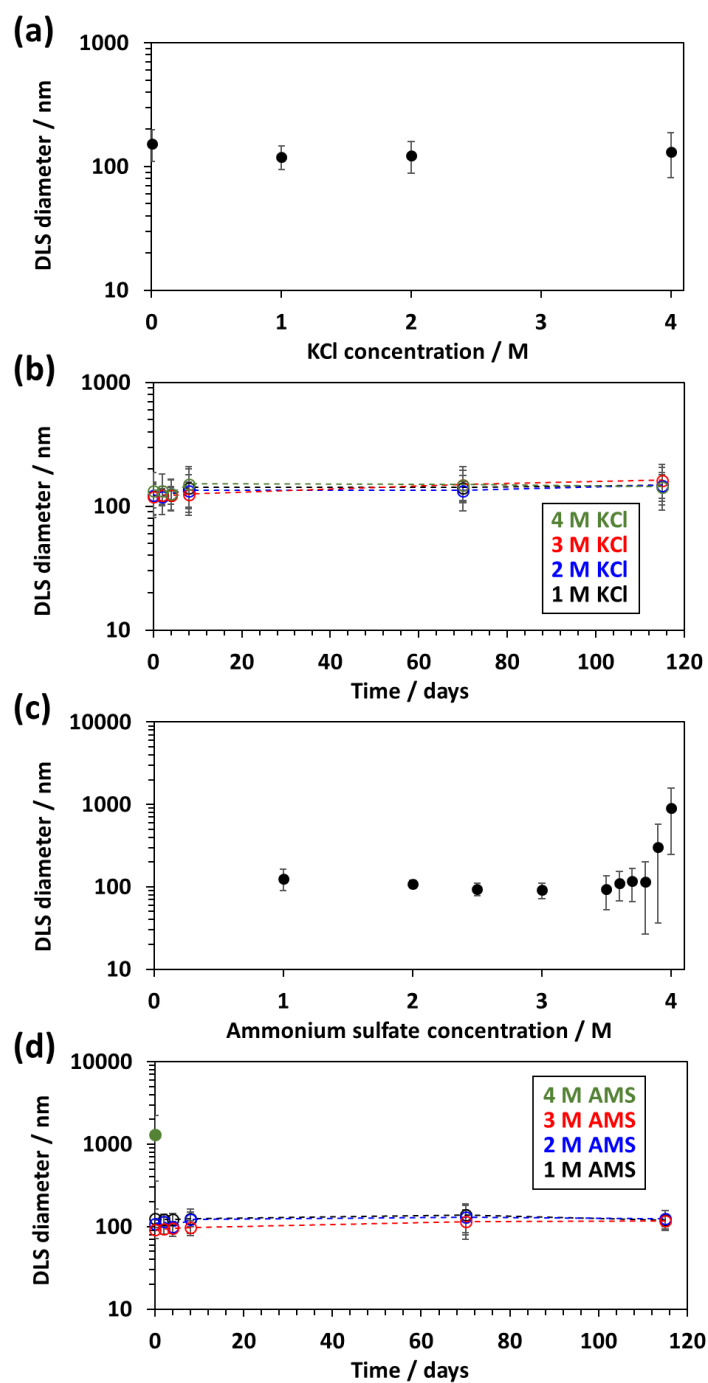
Fig. 4. (a + c) Plots of intensity-average DLS diameter against salt concentration for 0.1 % w/w aqueous dispersions of PATAC$_{100}$-PDAAM$_{1500}$ nanoparticles prepared using aqueous KCl or ammonium sulfate solutions respectively, ranging from 1.0 mM to 4.0 M (Standard deviations are calculated from the DLS PDI). **(b + d)** Plots of intensity-average DLS diameter against time for 0.1 % w/w aqueous dispersions of PATAC$_{100}$-PDAAM$_{1500}$ nanoparticles prepared using aqueous KCl or ammonium sulfate (AMS) solutions respectively, ranging from 1.0 M to 4.0 M. The dispersions were mixed at 20 ˚C for 115 days.

Aqueous electrophoresis measurements were conducted on 0.1 % w/w aqueous dispersions of PATAC$_{100}$-PDAAM$_{1500}$ nanoparticles in the presence of 0.0005 to 4.0 M KCl, see Figure 5. Initially, highly cationic zeta potentials ($\geq$ +35 mV) are observed at low salt concentrations (up to 0.1 M KCl) and are reduced monotonically to less than +10 mV at 4 M KCl. Similar observations were reported by Garg et al.,[58] who used optical microelectrophoresis to determine the electrophoretic mobilities of ~3 μm amidinated or sulfated polystyrene latexes dispersed in highly salty aqueous media. Although the reduction in zeta potential with increasing salt concentration suggests substantial charge screening under such high salinity conditions, the validity of using the Smoluchowski model to calculate zeta potential from electrophoretic mobility is questionable and this approach most likely underestimates the true zeta potential.
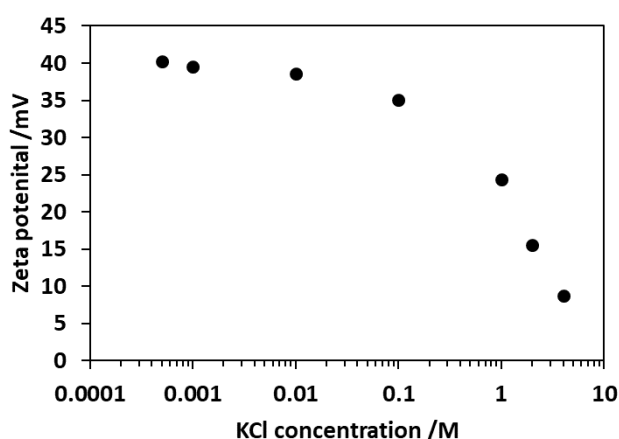

Fig. 5. Zeta potential data vs. KCl concentration determined for a 0.1% w/w aqueous dispersion of PATAC$_{100}$-PDAAM$_{1500}$ nanoparticles using an NG-ELS instrument.

Systematic variation of the mole fraction of PATAC stabilizer within the nanoparticles

On systematically varying n from 0.00 to 1.00 at a fixed z value of 1500, the zeta potential determined at pH 7 increased from essentially zero (+1 mV) when using the non-ionic

$PDMAC_{67}$ stabilizer block alone to +16 mV at n = 0.10, +28 mV at n = 0.25 and +32 mV at n = 0.50 (see entries 6 and 8 – 12 in Table 1). Thereafter, no significant change in zeta potential was observed for the 0.50 < n ≤ 1.00 interval. Clearly, incorporating further cationic $PATAC_{100}$ chains into the sterically-stabilized nanoparticles has no discernible additional effect on their electrophoretic behavior. For entries 8-12 in Table 1, smaller spheres are obtained as n is systematically varied from 0.0 to 0.75, with a concomitant increase in zeta potential from +1 to +38 mV. This suggests that the mutual electrostatic repulsion between neighboring cationic PATAC stabilizer chains leads to a lower mean aggregation number when a higher proportion of this component is used for these PISA syntheses. The salt resistance of a series of aqueous dispersions of (n $PATAC_{100}$ + (1-n) $PDMAC_{67}$)-$PDAAM_{1500}$ nanoparticles was examined when varying n from 0.00 to 1.00. As-synthesized 20 % w/w nanoparticle dispersions were diluted to 0.1% w/w using aqueous KCl solutions ranging from 1 mM up to 4.0 M, see Figure 6.
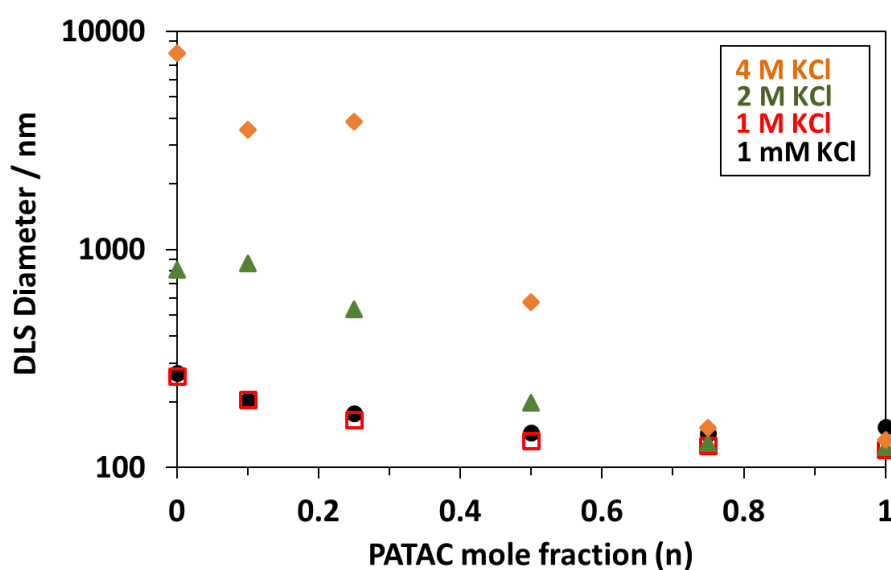

Fig. 6. Apparent DLS diameters determined for 0.1 % w/w aqueous dispersions of (n $PATAC_{100}$ + (1-n) $PDMAC_{67}$)-$PDAAM_{1500}$ spherical nanoparticles freshly dispersed in either 0.001, 1.0, 2.0 or 4.0 M KCl, where n is varied from 0.00 to 1.00.

In all cases, the (n PATAC$_{100}$ + (1-n) PDMAC$_{67}$)-PDAAM$_{1500}$ nanoparticles proved to be colloidally stable on dilution with 1.0 M KCl within 10 min of their addition to the concentrated salt solution, see Figure 6. However, only those nanoparticles containing a relatively high proportion of cationic PATAC stabilizer chains (i.e. n = 0.75 or n = 1.00) remained colloidally stable when diluted using 2.0 or 4.0 M KCl, see Figure 6. This is perhaps surprising given the relatively high cationic zeta potentials determined in the presence of 1 mM KCl for those nanoparticles prepared using n $\geq$ 0.25. This suggests that the colloidal stability depends on a sufficiently high charge density within the coronal stabilizer layer, rather than the nanoparticle zeta potential.

Salt tolerance of cationic block copolymer worms and vesicles

The synthesis of so-called 'higher order' morphologies such as worms and vesicles via PISA requires the efficient 1D fusion of spheres on the time scale of the RAFT dispersion polymerization.[28,29,35,59] Since electrosteric stabilization strongly inhibits such sphere-sphere fusion events, it is inherently difficult to produce worms and vesicles by chain extension of a polyelectrolytic homopolymer precursor.[46,47] However, worms and vesicles can be readily produced by chain extension of a judicious binary mixture of cationic and non-ionic precursors.[48,49] In the present study, it was found empirically that a somewhat shorter PDMAC stabilizer block was also required to allow access to higher order morphologies. Thus, chain extension of a binary mixture of 0.90 PDMAC$_{37}$ and 0.10 PATAC$_{100}$ targeting PDAAM DPs of 300 to 900 resulted in the formation of a series of well-defined vesicles (entries 14-16, Table 1, see Figure 7 for representative TEM images). Despite the relatively low PATAC$_{100}$ stabilizer density within the coronal layer, such vesicles proved to be highly cationic, with zeta potentials ranging from +34 mV to +40 mV. The (0.10 PATAC$_{100}$ + 0.90 PDMAC$_{37}$)-PDAAM$_{900}$ vesicles were selected for salt tolerance studies. An as-synthesized 20 % w/w dispersion was diluted to 0.1% w/w using a series of aqueous KCl solutions ranging from 1 mM to 4.0 M. The DLS data

indicate that these cationic vesicles remained reasonably stable in the presence of up to 1.0 M KCl but significant flocculation was observed at higher salt concentrations, see Figure 7d. This is not surprising given that markedly lower salt tolerance was also observed for cationic spheres prepared using a binary mixture of 0.10 PATAC and 0.90 PDMAC stabilizer blocks (see Figure 6).
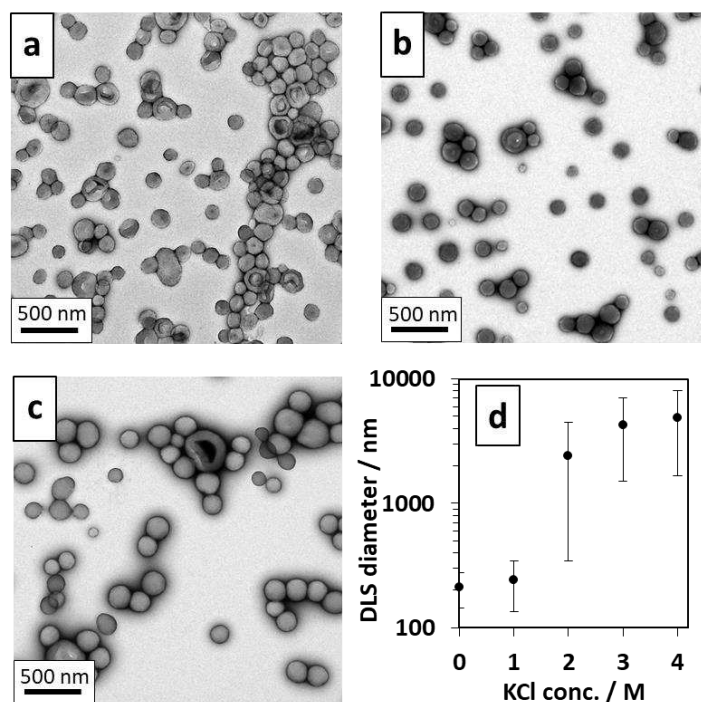

Fig. 7. Representative TEM images obtained for (a) (0.10 $PATAC_{100}$ + 0.90 $PDMAC_{37}$)-$PDAAM_{300}$ vesicles, (b) (0.10 $PATAC_{100}$ + 0.90 $PDMAC_{37}$)-$PDAAM_{600}$ vesicles and (c) (0.10 $PATAC_{100}$ + 0.90 $PDMAC_{37}$)-$PDAAM_{900}$ vesicles d) Apparent DLS diameter against KCl concentration for a 0.1% w/w dispersion of (0.10 $PATAC_{100}$ + 0.90 $PDMAC_{37}$)-$PDAAM_{900}$ vesicles prepared by diluting the as-synthesized 20% w/w vesicle dispersion using a series of aqueous KCl solutions.

Cationic worms could also be prepared by using a binary mixture of 0.10 $PATAC_{91}$ and 0.90 $PDMAC_{37}$ precursors to target a PDAAM DP of 90. As expected, these worms formed a free-

standing gel owing to multiple inter-worm contacts.[60] Such worms proved to be highly cationic with a zeta potential of +33 mV being observed in 1 mM KCl (see entry 13, Table 1). A representative TEM image is provided in Figure 8a. The salt tolerance of these (0.10 $PATAC_{91}$ + 0.90 $PDMAC_{37}$)-$PDAAM_{90}$ worms was assessed by DLS, see Figure 8. The as-synthesized 20 % w/w worm dispersion was diluted to 0.1% w/w using aqueous KCl solutions ranging from 1 mM to 4.0 M and mixed for 10 min prior to analysis. The worms remained colloidally stable up to 2.0 M KCl, with significant flocculation being observed at higher salt concentrations.
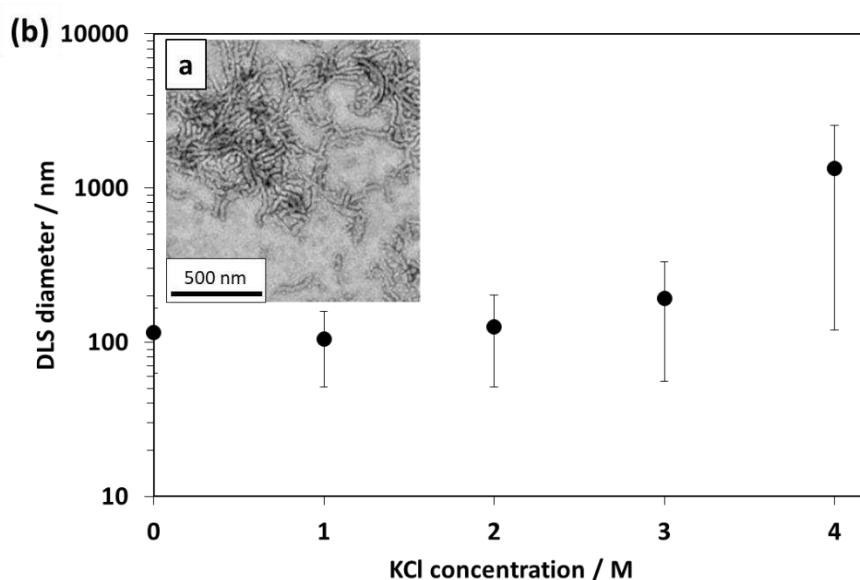

Fig. 8. Apparent DLS diameter against KCl concentration for a 0.1% w/w aqueous dispersion of (0.1 $PATAC_{91}$ + 0.9 $PDMAC_{37}$)-$PDAAM_{90}$ worms prepared by diluting the as-synthesized 20% w/w worm dispersion using a series of aqueous KCl solutions.

Conclusions

A series of new cationic diblock copolymer spherical nanoparticles have been prepared via RAFT aqueous dispersion polymerization of DAAM using either a quaternized PATAC

precursor as a steric stabilizer block or a binary mixture of this cationic precursor plus a non-ionic PDMAC steric stabilizer. These nanoparticles exhibited surprisingly strong resistance towards flocculation in highly salty aqueous media. In particular, DLS studies confirmed that highly cationic spheres prepared using PATAC as the sole steric stabilizer remained colloidally stable in the presence of either 4.0 M KCl or 3.5 M ammonium sulfate for almost four months when stored at 20 °C. However, spheres prepared using binary mixtures of both PATAC and PDMAC stabilizer blocks proved to be significantly less tolerant towards added salt, despite exhibiting similarly cationic zeta potentials. Thus the latter parameter is not necessarily a good predictor of salt tolerance for such colloidal dispersions. Moreover, cationic block copolymer worms and vesicles could also be prepared using this PISA formulation by utilizing a relatively low mole fraction of the cationic PATAC block as a steric stabilizer. These latter dispersions also exhibited reasonably good salt tolerance, with worms retaining their colloidal stability in the presence of up to 2.0 M KCl while vesicles resisted flocculation up to 1.0 M KCl. Such nanoparticles are likely to be excellent model systems for understanding the behavior of aqueous colloidal dispersions in the presence of relatively high concentrations of electrolyte. Finally, we report for the first time the use of a next-generation ELS instrument to determine the zeta potential of nanoparticles dispersed in highly salty media.

Acknowledgments

Supporting Information Available.

^1H NMR and uv/visible absorption spectra for the Me-DDMAT RAFT agent. Aqueous GPC traces recorded for the $PATAC_{91}$ and $PATAC_{100}$ homopolymer precursors. DMF GPC traces recorded for the $PDMAC_{37}$ and $PDMAC_{67}$ homopolymer precursors. ^1H NMR spectrum recorded for the $(0.1\ PATAC_{100} + 0.9\ PDMAC_{67})\text{-}PDAAM_{1500}$ diblock copolymer. A summary table of KCl and ammonium sulfate solution viscosities used for DLS analysis at 20 °C.

References

(1)   Selmi, F. Studi Sulla Dimensione Di Cloruro d'argento. Nuovi Ann. delle Sci. Nat. di Bol. **1845**, IV, 146.

(2)   Graham, T. On the Properties of Silicic Acid and Other Analogous Colloidal Substances. J. Chem. Soc. **1864**, No. 17, 318–327.

(3)   Derjaguin, B.; Landau, L. Theory of the Stability of Strongly Charged Lyophobic Sols and of the Adhesion of Strongly Charged Particles in Solution of Electrolytes. Acta Physicochim. U.R.S.S **1941**, 14, 633–662.

(4)   Verwey, E.; Overbeek, Jt. Theory of the Stability of Lyophobic Colloids; Elsevier: Amsterdam, 1948.

(5)   Groves, R.; Routh, A. F. Film Deposition and Consolidation during Thin Glove Coagulant Dipping. J. Polym. Sci. Part B Polym. Phys. **2017**, 55 (22), 1633–1648.

(6)   Faraday, M. The Bakerian Lecture - Experimental Relations of Gold (and Other Metals) to Light. Philos. Trans. R. Soc. A **1857**, 147, 145–181.

(7)   Kotsmar, C.; Yoon, K. Y.; Yu, H.; Ryoo, S. Y.; Barth, J.; Shao, S.; Prodanović, M.; Milner, T. E.; Bryant, S. L.; Huh, C.; et al. Stable Citrate-Coated Iron Oxide Superparamagnetic Nanoclusters at High Salinity. Ind. Eng. Chem. Res. **2010**, 49 (24), 12435–12443.

(8)   Hwang, C. C.; Wang, L.; Lu, W.; Ruan, G.; Kini, G. C.; Xiang, C.; Samuel, E. L. G.; Shi, W.; Kan, A. T.; Wong, M. S.; et al. Highly Stable Carbon Nanoparticles Designed for Downhole Hydrocarbon Detection. Energy Environ. Sci. **2012**, 5 (8), 8304–8309.

(9)   Bagaria, H. G.; Yoon, K. Y.; Neilson, B. M.; Cheng, V.; Lee, J. H.; Worthen, A. J.; Xue, Z.; Huh, C.; Bryant, S. L.; Bielawski, C. W.; et al. Stabilization of Iron Oxide Nanoparticles in High Sodium and Calcium Brine at High Temperatures with Adsorbed Sulfonated Copolymers. Langmuir **2013**, 29 (10), 3195–3206.

(10)   Bagaria, H. G.; Xue, Z.; Neilson, B. M.; Worthen, A. J.; Yoon, K. Y.; Nayak, S.; Cheng, V.; Lee, J. H.; Bielawski, C. W.; Johnston, K. P. Iron Oxide Nanoparticles Grafted with Sulfonated Copolymers Are Stable in Concentrated Brine at Elevated Temperatures and Weakly Adsorb on Silica. ACS Appl. Mater. Interfaces **2013**, 5 (8), 3329–3339.

(11)   Kini, G. C.; Yu, J.; Wang, L.; Kan, A. T.; Biswal, S. L.; Tour, J. M.; Tomson, M. B.; Wong, M. S. Salt- and Temperature-Stable Quantum Dot Nanoparticles for Porous

Media Flow. Colloids Surfaces A Physicochem. Eng. Asp. **2014**, 443, 492–500.

(12) Ranka, M.; Brown, P.; Hatton, T. A. Responsive Stabilization of Nanoparticles for Extreme Salinity and High-Temperature Reservoir Applications. ACS Appl. Mater. Interfaces **2015**, 7 (35), 19651–19658.

(13) Sun, X.; Zhang, Y.; Chen, G.; Gai, Z. Application of Nanoparticles in Enhanced Oil Recovery: A Critical Review of Recent Progress. Energies **2017**, 10 (3), 345.

(14) Cho, M. S.; Yoon, K. J.; Song, B. K. Dispersion Polymerization of Acrylamide in Aqueous Solution of Ammonium Sulfate : Synthesis and Characterisation. J. Appl. Polym. Sci. **2002**, 83, 1397–1405.

(15) Aijun, G.; Yiran, G.; Lili, Z.; Jun, L.; Dong, L.; Peng, L. Preparation of Cationic Polyacrylamide Microsphere Emulsion and Its Performance for Permeability Reduction. Pet. Sci. **2014**, 11, 408–416.

(16) Chiefari, J.; Chong, Y. K. B.; Ercole, F.; Krstina, J.; Jeffery, J.; Le, T. P. T.; Mayadunne, R. T. A.; Meijs, G. F.; Moad, C. L.; Moad, G.; et al. Living Free-Radical Polymerization by Reversible Addition-Fragmentation Chain Transfer: The RAFT Process. Macromolecules **1998**, 31, 5559–5562.

(17) Qiu, J.; Charleux, B.; Matyjaszewski, K. Controlled/Living Radical Polymerization in Aqueous Media: Homogeneous and Heterogeneous Systems. Prog. Polym. Sci. **2001**, 26, 2083–2134.

(18) Hill, M. R.; Carmean, R. N.; Sumerlin, B. S. Expanding the Scope of RAFT Polymerization: Recent Advances and New Horizons. Macromolecules **2015**, 48 (16), 5459–5469.

(19) Zhou, W.; Qu, Q.; Xu, Y.; An, Z. Aqueous Polymerization-Induced Self-Assembly for the Synthesis of Ketone-Functionalized Nano-Objects with Low Polydispersity. ACS Macro Lett. **2015**, 4, 495–499.

(20) Mitsukami, Y.; Donovan, M. S.; Lowe, A. B.; McCormick, C. L. Water-Soluble Polymers. 81. Direct Synthesis of Hydrophilic Styrenic-Based Homopolymers and Block Copolymers in Aqueous Solution via RAFT. Macromolecules **2001**, 34 (7), 2248–2256.

(21) Lai, J. T.; Filla, D.; Shea, R. Functional Polymers from Novel Carboxyl-Terminated Trithiocarbonates as Highly Efficient RAFT Agents. Am. Chem. Soc. Polym. Prepr. Div. Polym. Chem. **2002**, 35, 6754–6756.

(22) McCormick, C. L.; Lowe, A. B. Aqueous RAFT Polymerization: Recent Developments in Synthesis of Functional Water-Soluble (Co)Polymers with Controlled Structures. Acc. Chem. Res. **2004**, 37 (5), 312–325.

(23) Moad, G.; Rizzardo, E.; Thang, S. H. Living Radical Polymerization by the RAFT Process. Aust. J. Chem. **2005**, 58, 379–410.

(24) Perrier, S.; Takolpuckdee, P. Macromolecular Design via Reversible Addition-Fragmentation Chain Transfer (RAFT)/Xanthates (MADIX) Polymerization. J. Polym. Sci. Part A Polym. Chem. **2005**, 43 (22), 5347–5393.

(25) Lowe, A. B.; McCormick, C. L. Reversible Addition-Fragmentation Chain Transfer (RAFT) Radical Polymerization and the Synthesis of Water-Soluble (Co)Polymers

under Homogeneous Conditions in Organic and Aqueous Media. Prog. Polym. Sci. **2007**, 32 (3), 283–351.

(26) Zetterlund, P. B.; Kagawa, Y.; Okubo, M. Controlled/Living Radical Polymerization in Dispersed Systems. Chem. Rev. **2008**, 108, 3747–3794.

(27) Zhang, X.; Boissé, S.; Zhang, W.; Beaunier, P.; D'Agosto, F.; Rieger, J.; Charleux, B. Well-Defined Amphiphilic Block Copolymers and Nano-Objects Formed in Situ via RAFT-Mediated Aqueous Emulsion Polymerization. Macromolecules **2011**, 44 (11), 4149–4158.

(28) Canning, S. L.; Smith, G. N.; Armes, S. P. A Critical Appraisal of RAFT-Mediated Polymerization-Induced Self-Assembly. Macromolecules **2016**, 49, 1985–2001.

(29) Warren, N. J.; Armes, S. P. Polymerization-Induced Self-Assembly of Block Copolymer Nano-Objects via RAFT Aqueous Dispersion Polymerization. J. Am. Chem. Soc. **2014**, 136, 10174–10185.

(30) Charleux, B.; Delaittre, G.; Rieger, J.; D'Agosto, F. Polymerization-Induced Self-Assembly: From Soluble Macromolecules to Block Copolymer Nano-Objects in One Step. Macromolecules **2012**, 45 (17), 6753–6765.

(31) Derry, M. J.; Fielding, L. A.; Armes, S. P. Polymerization-Induced Self-Assembly of Block Copolymer Nanoparticles via RAFT Non-Aqueous Dispersion Polymerization. Prog. Polym. Sci. **2016**, 52, 1–18.

(32) Tan, J.; Sun, H.; Yu, M.; Sumerlin, B. S.; Zhang, L. Photo-PISA: Shedding Light on Polymerization-Induced Self-Assembly. ACS Macro Lett. **2015**, 4 (11), 1249–1253.

(33) Jiang, Y.; Xu, N.; Han, J.; Yu, Q.; Guo, L.; Gao, P.; Lu, X.; Cai, Y. The Direct Synthesis of Interface-Decorated Reactive Block Copolymer Nanoparticles via Polymerisation-Induced Self-Assembly. Polym. Chem. **2015**, 6, 4955–4965.

(34) Zhou, D.; Dong, S.; Kuchel, R. P.; Perrier, S.; Zetterlund, P. B. Polymerization Induced Self-Assembly: Tuning of Morphology Using Ionic Strength and PH. Polym. Chem. **2017**, 8 (20), 3082–3089.

(35) Khor, S. Y.; Quinn, J. F.; Whittaker, M. R.; Truong, N. P.; Davis, T. P. Controlling Nanomaterial Size and Shape for Biomedical Applications via Polymerization-Induced Self-Assembly. Macromol. Rapid Commun. **2019**, 40 (2), 1–22.

(36) Karagoz, B.; Esser, L.; Duong, H. T.; Basuki, J. S.; Boyer, C.; Davis, T. P. Polymerization-Induced Self-Assembly (PISA)-Control over the Morphology of Nanoparticles for Drug Delivery Applications. Polym. Chem. **2014**, 5 (2), 350–355.

(37) Byard, S. J.; Williams, M.; Mckenzie, B. E.; Blanazs, A.; Armes, S. P. Preparation and Cross-Linking of All-Acrylamide Diblock Copolymer Nano-Objects via Polymerization-Induced Self-Assembly in Aqueous Solution. Macromolecules **2017**, 50, 1482–1493.

(38) Skrabania, K.; Miasnikova, A.; Bivigou-Koumba, A. M.; Zehm, D.; Laschewsky, A. Examining the UV-Vis Absorption of RAFT Chain Transfer Agents and Their Use for Polymer Analysis. Polym. Chem. **2011**, 2, 2074–2083.

(39) Weast, R. Handbook of Chemistry and Physics, 66th Editi.; CRC Press: Florida.

(40) Uzgiris, E. Laser Doppler Spectroscopy: Applications to Cell and Particle Electrophoresis. Adv. Colloid Interface Sci. **1981**, 14, 75–171.

(41) Miller, J. Measuring Electrophoretic Mobility. WO20190011398, 2019.

(42) Miller, J. F.; Schätzel, K.; Vincent, B. The Determination of Very Small Electrophoretic Mobilities in Polar and Nonpolar Colloidal Dispersions Using Phase Analysis Light Scattering. J. Colloid Interface Sci. **1991**, 143 (2), 532–554.

(43) Feltham, A. M.; Spiro, M. Platinized Platinum Electrodes. Chem. Rev. **1971**, 71 (2), 177–193.

(44) Hunter, R. Zeta Potential in Colloid Science; Academic Press: London, 1981.

(45) Blanazs, A.; Ryan, A. J.; Armes, S. P. Predictive Phase Diagrams for RAFT Aqueous Dispersion Polymerization: Effect of Block Copolymer Composition, Molecular Weight, and Copolymer Concentration. Macromolecules **2012**, 45, 5099–5107.

(46) Semsarilar, M.; Ladmiral, V.; Blanazs, A.; Armes, S. P. Anionic Polyelectrolyte-Stabilized Nanoparticles via RAFT Aqueous Dispersion Polymerization. Langmuir **2012**, 28 (24), 914–922.

(47) Semsarilar, M.; Ladmiral, V.; Blanazs, A.; Armes, S. P. Cationic Polyelectrolyte-Stabilized Nanoparticles via RAFT Aqueous Dispersion Polymerization. Langmuir **2013**, 29 (24), 7416–7424.

(48) Williams, M.; Penfold, N. J. W.; Lovett, J. R.; Warren, N. J.; Douglas, C. W. I.; Doroshenko, N.; Verstraete, P.; Smets, J.; Armes, S. P. Bespoke Cationic Nano-Objects via RAFT Aqueous Dispersion Polymerisation. Polym. Chem. **2016**, 7, 3864–3873.

(49) Penfold, N.; Ning, Y.; Verstraete, P.; Smets, J.; Armes, S. P. Cross-Linked Cationic Diblock Copolymer Worms Are Superflocculants for Micrometer-Sized Silica Particles. Chem. Sci. **2016**.

(50) Chaduc, I.; Girod, M.; Antoine, R.; Charleux, B.; D'Agosto, F.; Lansalot, M. Batch Emulsion Polymerization Mediated by Poly(Methacrylic Acid) MacroRAFT Agents: One-Pot Synthesis of Self-Stabilized Particles. Macromolecules **2012**, 45 (15), 5881–5893.

(51) Buffle, J.; van Leeuwen, H. Environmental Particles; Lewis Publishers: New York, 1993.

(52) Munro, D.; Goodall, A. R.; Wilkinson, M. C.; Randle, K.; Hearn, J. Study of Particle Nucleation, Flocculation, and Growth in the Emulsifier-Free Polymerization of Styrene in Water by Total Intensity Light Scattering and Photon Correlation Spectroscopy. J. Colloid Interface Sci. **1979**, 68 (1), 1–13.

(53) Weitz, D.; Huang, J.; Lin, M.; Sung, J. Dynamics of Diffusion-Limited Kinetic Aggregation. Phys. Rev. Lett. **1984**, 53 (17), 1657–1660.

(54) Ditsch, A.; Laibinis, P. E.; Wang, D. I. C.; Hatton, T. A. Controlled Clustering and Enhanced Stability of Polymer-Coated Magnetic Nanoparticles. Langmuir **2005**, 21 (13), 6006–6018.

(55) Gregory, J. Monitoring Particle Aggregation Processes. Adv. Colloid Interface Sci.

2009, 147–148, 109–123.

(56) Fuoss, R. M.; Strauss, U. P. Electrostatic Interaction of Polyelectrolytes and Simple Electrolytes. J. Polym. Sci. **1948**, 3 (4), 602–603.

(57) Lewis, G. N.; Randall, M. The Activity Coefficient of Strong Electrolytes. J. Am. Chem. Soc. **1921**, 43 (5), 1112–1154.

(58) Garg, A.; Cartier, C. A.; Bishop, K. J. M.; Velegol, D. Particle Zeta Potentials Remain Finite in Saturated Salt Solutions. Langmuir **2016**, 32 (45), 11837–11844.

(59) Blanazs, A.; Madsen, J.; Battaglia, G.; Ryan, A. J.; Armes, S. P. Mechanistic Insights for Block Copolymer Morphologies: How Do Worms Form Vesicles? J. Am. Chem. Soc. **2011**, 133, 16581–16587.

(60) Lovett, J. R.; Derry, M. J.; Yang, P.; Hatton, F. L.; Warren, N. J.; Fowler, P. W.; Armes, S. P. Can Percolation Theory Explain the Gelation Behavior of Diblock Copolymer Worms? Chem. Sci. **2018**, 9, 7138–7144.

For Table of Contents Only

Cationic sterically-stabilized diblock copolymer nanoparticles exhibit exceptional tolerance towards added salt

Sarah J. Byard, Adam Blanazs, John F. Miller and Steven P. Armes*